Metabolomic Characteristics of Solid Pseudopapillary Tumor of the Pancreas: Relationship with high intensity ^{18}F-FDG PET-Scan

Chang Moo Kang

Department of Medicine

The Graduate School, Yonsei University

Metabolomic Characteristics of Solid Pseudopapillary Tumor of the Pancreas: Relationship with high intensity ^{18}F-FDG PET-Scan

Directed by Professor Woo Jung Lee

The Doctoral Dissertation
submitted to the Department of Medicine,
The Graduate School of Yonsei University
in partial fulfillment of the requirements for the degree
of Doctor of Philosophy

Chang Moo Kang

June 2014

This certifies that the Doctoral Dissertation of Chang Moo Kang is approved.

Thesis Supervisor : Woo Jung Lee

Thesis Committee Member#1 : Jin Sub Choi

Thesis Committee Member#2 : Kyung Sub Kim

Thesis Committee Member#3 : Seung Woo Park

Thesis Committee Member#4 : Song Cheol Kim

The Graduate School
Yonsei University

June 2014

ACKNOWLEDGEMENTS

"*To have knowledge, you must first have reverence for the LORD."* *PROVERBS 1:7*

It was a really long and unpleasant 'Journey'. The way was not straight, not simple, and not that easy. It was paved with dusts and frustrations. I felt that I was totally helpless and alone. During the Journey of preparing my doctoral thesis, only my scientific knowledge but also spirituality has grown up. I realized the LORD had already prepared for everything for me. He provided me with what I exactly needed. He, again, reminded me of 'Immanuel' in my life. I was not alone, and I am not alone, neither.

First of all, I would like to express special thanks to my wife, Kyung Hee and my lovely daughter, Hera. Without their love and emotional support, I'm not definitely sure that I could have finished this work. I also appreciate all my family members including my father, my elder sisters, and my parents-in-law, who always prayed for and took care of me. I deeply thank thesis supervisor, Professor Woo Jung Lee, as well as all thesis committee members, Professor Jin Sub Choi, Professor Kyung Sup Kim, professor Seung Woo Park, and Professor Song Cheol Kim. I believe this thesis could be improved by their thoughtful advices and academic comments based on their expertise in both clinical and basic research

field. Especially, I also appreciate Professor Hoguen Kim. As my mentor since I was a medical student, he gave me lots of priceless comments and wisdom for this study. Without his special support, I could not have completed the present study. Finally, I would like to thank Professor Se Hoon Kim, for teaching important technical tips for preparing manuscript.

This would not be the end of my ‘Journey’, but a small part of it. More tough and rough path may come (No doubt about it!). But, I know I will not be alone. My LORD always has taken, is taking, and will take care of me forever. I’m not afraid.

30th June, 2014

<TABLE OF CONTENTS>

LIST OF FIGURES

LIST OF TABLES

LIST OF SUPPLEMENTARIES

ABSTRACT

Metabolomic Characteristics of Solid Pseudopapillary Tumor of the Pancreas: Relationship with high intensity ^{18}F-FDG PET-Scan

Chang Moo Kang

Department of Medicine
The Graduate School, Yonsei University

(Directed by Professor Woo Jung Lee)

Introduction: Solid pseudopapillary tumor (SPT) of the pancreas is a very rare pathologic condition occurring predominantly in female patients. Surgical resection is only way to cure of the disease, but the origin of the tumor and natural course of the disease are still unknown. Recently, ^{18}F-FDG PET / PET-CT scan has been widely applied for differential diagnosis, preoperative staging, and determining treatment effect. Only a few literatures investigated the appearances of SPTs on ^{18}F-FDG PET / PET-CT scan. However, there is no study to define the patterns of SPT on ^{18}F-FDG PET / PET-CT scan, and to reveal metabolomics characteristics explaining high ^{18}F-FDG uptake in SPT of the pancreas.

Methods: mRNA expression for glucose metabolism was checked from 5 samples of SPT, pancreatic ductal adenocarcinoma (PCA), and paired normal pancreatic tissues. Differentially expressed genes between non-neoplastic pancreatic tissue and pancreatic tumors (SPN, or PCA) were determined as those with $p<0.01$ and a fold change >1.5. The expressions of selected genes for glucose metabolism in SPT were also confirmed by both western bolt and immunohistochemistry. Medical

records of the patients with SPT who underwent pancreatectomy were retrospectively reviewed. Among them, 36 patients with preoperative ^{18}F-FDG PET scan were selected. Clinical pattern of clinical pattern of SPT on ^{18}F-FDG PET / PET-CT scan were classified according to the proportion of ^{18}F-FDG uptake within the whole tumor volume (hot uptake: ≥70%, mixed: 30≤ <70, and defective: <30%). PET-based parameters, such as maximum standardized uptake value (SUV_{max}), mean standardized uptake value (SUV_{mean}), metabolic tumor volume ($TMV_{2.5}$), and total lesion glycolysis ($TLG_{2.5}$) were evaluated. Correlation between pattern of ^{18}F-FDG uptake, expression of glucose metabolism-related genes, and microscopic malignant features was performed.

Results: Thirty-five patients (97.2%) were female and only one was male with age, 34.8±11.2 years. Clinical patterns of ^{18}F-FDG uptake were categorized into three types; hot-uptake (N=19), mixed (N=5), and defective type (N=12). Radiologic tumor size, SUV_{max}, SUV_{mean}, and $TLG_{2.5}$ were significant different according to pattern of ^{18}F-FDG uptake (ANOVA, $p<0.05$). It was observed that glucose metabolism-related genes, such as GLUT1, HK1, PFKM, ENO2, PKM2 were highly expressed in SPTs in both mRNA and protein level. Comparing with hot+mixed type, defective type of SPTs showed lower expression of HK1 (p=0.014), PKM2 (p=0.028), and Ki-67 (p=0.070) with frequent intratumoral necrosis (p=0.007). High Ki-67 expression (≥3%) was associated with high SUV_{max} of SPT of the pancreas (p=0.002). In addition, defective type of SPT tended to be associated with benign microscopic features (p=0.070). In literatures review, hot+

mixed type of SPTs appeared to be more aggressive comparing to defective type of SPTs.

Conclusion: This study is the first investigation to dissect metabolomic characteristics of SPT of the pancreas. Basically, SPT cells harbor active molecular capacity for increasing glucose metabolism, and it was well visualized in ^{18}F-FDG-PET/ PET-CT scan. Therefore, clinical patterns of ^{18}F-FDG uptake in SPTs can be influenced according to intratumoral hemorrhagic necrosis and can be classified as three types; hot uptake, mixed, and defective type. Form the view point of metabolomics, defective type of SPTs was associated with low metabolic activity and apparently related to low Ki-67 index, suggesting there is some room for reserving surgery in this type of SPTs. Further study needs to be conducted to identify metabolomics differences between indolent and aggressive STPs of the pancreas.

Key words: Solid pseudopapillary tumor, metabolomics, metabolism, ^{18}floro-deoxyglucose positron emission tomography (^{18}F-FDG-PET), pancreatectomy

Metabolomic Characteristics of Solid Pseudopapillary Tumor of the Pancreas: Relationship with high intensity ^{18}F-FDG PET-Scan

Chang Moo Kang

Department of Medicine
The Graduate School, Yonsei University

(Directed by Professor Woo Jung Lee)

I. INTRODUCTION

Solid pseudopapillary tumor (SPT) is very rare pathologic conditions of the pancreas. It comprised only 1-3% of all exocrine pancreatic tumors, and 6-12% of cystic tumors of the pancreas. In spite of clinical rarity of this pathologic condition, its clinical recognition and concerns as differential diagnosis have increased. In fact, a recent Korean nationwide survey of cystic neoplasm of the exocrine pancreas[1] revealed that SPTs were the third most common (18.3%, 195 out of 1064 patients), which indicates that pancreatic SPTs may not be uncommon in Korea. This tumor is also known as Frantz tumor[2], named after the author's name who first discovered the characteristics of this tumor. Hamoudi, et al[3] added additional patients and described detailed microscopic appearance of the tumor in 1970. Since then, various names have been used to describe this lesion, such as "solid and papillary tumor[4]", "solid papillary-cystic tumor[5]", "papillary cystic tumor[6]", "solid-cystic tumor[7]", and "solid, cystic, and papillary epithelial neoplasm[8]". In 1996, it was finally included in the WHO classification of pancreatic tumors under the name of *solid pseudopapillary tumor*[9].

SPT predominantly affects young female patients. Reviewing 718 patients reported in English literatures[10], it was noted that only 64 patients were male

and the rest 626 were female (9.78:1) with mean age of 21.97 years (range, 2-85 years). Though these tumors are often found in large tumor size, most SPTs are well circumscribed and surgical resection usually shows an excellent prognosis**.** It was reported that approximately 10 to 15% of cases of SPTs are malignant, but complete surgical resection of these tumors can promise long-term survival even in cases of distant metastasis and peritoneal seeding[6,11-13], suggesting local invasion, tumor recurrence, distant metastasis, and peritoneal seeding should not be contraindication for potential cure of the disease.

Although additional genetic analysis is required to identify the exact mechanism for tumorigenesis of SPT, it was recently found that SPTs have β-catenin gene mutation.[14,15] Diffuse cytoplasmic and nuclear localization for β-catenin is almost found in SPT. β-catenin functions as a downstream transcriptional co-activiator in the Wint signaling pathway; therefore, the Wnt signal pathway is thought to play an important role in tumorigenesis of SPT. In normal epithelial cells, β-catenin is present in a submembranous location and the levels of cytoplasmic β-catenin are very low because β-catenin is phosphorylated by a complex of the adenomatous polyposis coli tumor suppressor (APC), AXIN, and glycogen synthetase kinase-3β (GSK-3β) to be degraded in a ubiquitin-dependent proteasome system[16]. Under the condition of Wnt signal activation, or mutation in the APC gene, the AXIN, or the β-catenin gene itself, the phosphorylation of β-catenin by GSK-3β is inhibited, which results in high levels of β-catenin accumulation in the cytosol[17,18]. The accumulated β-catenin, in turn, binds to transcription factors, cytosolic T cell factor/ lymphoid-enhancer-factor (Tcf/Lef), translocates to the nucleus, and activates important Wnt target genes, such as MMP-7, cyclin-D1, and c-myc.[19-22] Abnormal cytoplasmic and nuclear β-catenin accumulation is already well-known in SPT of the pancreas, suggesting a role of the Wnt

signal pathway in the tumorigenesis of SPTs.[14,15,23]

However, there are several issues remain to be solved in SPT of the pancreas. First, the origin of SPTs is still controversial. Acinar[24,] centriacinar[25], ductal[24], endocrine[26,27], multipoint primordial cells[28,29] and neurocrest origins[30] have been proposed, but the exact histogenesis of this tumor remains to be determined. Second, the clinical course after complete tumor removal is unpredictable. No reliable pathologic factors that can predict the prognosis have been identified[31-33]. It has been suggested that microscopic features like perineural, vascular invasion, a high degree of cellular pleomorphism, an elevated mitotic rate, lymph node metastasis, and pancreatic parenchyma/ capsular invasion are associated with metastasis and recurrence (malignancy)[6,13,34-36]. However, its clinical course is known to be unpredictable because both pathological and biological prognostic factors are nonspecific for metastasis and recurrence[37]. Therefore, pancreatic SPTs have the nick name of "*surgical enigmas*"[32,38,39]

Back in the 1924, Otto Warburg found that normal cells mobilize glucose to mitochondrial oxidative phosphorylation to generate ATP when oxygen is abundant, but, tumor cells generally exhibit greater glucose uptake with increased glycolysis and lactate production, regardless of oxygen availability. It might be suggesting that this Warburg's effect[40] [aerobic glycolysis] is basically required for adequate supply of energetic and anabolic substrates for massive macromolecular biosynthesis in cancer cell. It has now become clear that the Warburg effect represents the metabolic rearrangements that accompany malignant transformation, which involving not only aerobic glycolysis but also an increased flux through the pentose phosphate pathway (PPP), elevated lipid biosynthesis, high glutamine consumption, maintenance of redox homeostasis[41-43](Fig. 1-(A)). This phenomenon formed the basis for the development of ^{18}floro-deoxyglucose positron emission tomography

(^{18}F-FDG-PET) for clinical application. ^{18}F-FDG-PET scan is an evolving diagnostic modality for tumor detection, differentiation between benign and malignant lesions, staging work-up, therapeutic monitoring, and following-up of various malignant conditions. It is the basic background that the enhanced glucose metabolism in cancer cell augments ^{18}F-FDG uptake into malignant tissue[44]. ^{18}F-FDG is a glucose derivative where the hydroxyl function in position 2 is replaced by the radioactive fluorine isotope. ^{18}F-FDG is transported into tumor cells with the aid of glucose transporters. Glucose transporter- 1(GLUT-1) was identified as principal glucose transporter[45] and hexokinases(HK), which were noted to be overexpressed in cancer cells, phosphorylate incorporated glucose and result in increased accumulation of phosphorylated ^{18}F-FDG within the tumor cells. Because of the missing hydroxyl function in position 2, subsequent metabolism via glucose-6-phosphate isomerase is not possible. Therefore, ^{18}F-FDG-6-phosphate is not further degraded. In addition, it cannot penetrate the cell membrane due to its negative charge, leading to the trapping in the cell [46-48] (Figure. 1-(B)). In tumor cells, it is known that glucose transport and metabolism is altered to increase ^{18}F-FDG uptake compared to normal cells.

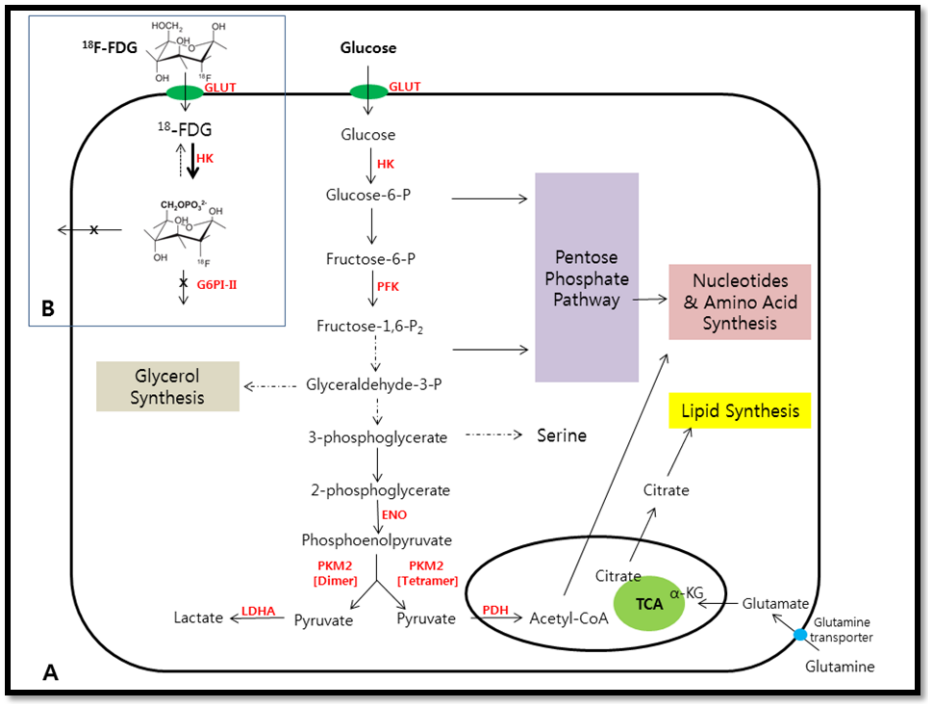

Figure 1 Glucose metabolism and principle of ^{18}F-FDG accumulation in tumor cell. Schematic illustration of tumor metabolism (A), and principal mechanism of ^{18}F-FDG uptake in PET scan (B)

The clinical and biological significance of ^{18}F-FDG PET scan have been investigated in many malignancies arising from gastrointestinal tract, however, only a few literatures are currently available dealing with the appearance of SPT on ^{18}F-FDG PET or PET/CT. According to clinical experiences and reported literatures[49-52], SPTs of the pancreas commonly represent high uptake of ^{18}F-FDG requiring differentiation from pancreatic cancer. However, it is quite rare to investigate the mechanism of ^{18}F-FDG uptake in SPT. In 2006, Sato, et al[53] showed that poor expression of GLUT-1 and moderate expression of HK-II on immunohistochemistry staining, suggesting that FDG accumulation might be related to tumor cell density and rich mitochondria in

SPT cells based on only two cases. In addition, ^{18}F-FDG PET scan can represent metabolic and biologic activity of the tumors, however, it only focuses on the initial steps of glucose metabolism, such as glucose transporter and hexokinase, not whole pathway of glucose metabolism in SPT of the pancreas. Therefore, in this study, we investigated metabolomics characteristics in SPT of the pancreas and correlated with signal intensity of ^{18}F-FDG PET scan.

II. MATERIALS AND METHODS

1. Patients' clinical data

The medical records of 36 patients with SPT who took preoperative ^{18}F-FDG PET/PET-CT scan and underwent pancreatectomy were retrospectively reviewed. The clinicopathologic characteristics of the patients, including age, gender, radiologic tumor size, and microscopic malignant features, were investigated.

2. ^{18}F-FDP PET/ PET-CT protocol

All ^{18}F-FDG PET/PET-CT scans were performed with a dedicated PET/CT scanner (Discovery STe, GE Healthcare; or Biograph TruePoint 40, Siemens Healthcare. All patients fasted for at least 6 h prior to the PET/CT scan. A dose of approximately 5.5 MBq/kg of ^{18}F-FDG was intravenously injected 60 min before imaging. First, a CT scan was performed at 30 mA and 130 kVp for Discovery STe, and 36 mA and 120 kVp for Biograph TruePoint without contrast-enhancement. After the CT scan was complete, a PET scan was performed extending from the neck to the proximal thighs with an acquisition time of 3 min per bed position in 3D mode. PET images were reconstructed using ordered subset expectation maximization (OSEM) with an attenuation correction.

3. Image evaluation and PET-based parameters

^{18}F-FDG PET/CT images were reviewed by two nuclear medicine physicians using an Advantage Workstation 4.4 (GE Medical Systems). Maximum standardized uptake value (SUV_{max}), mean SUV(SUV_{mean}), $MTV_{2.5}$, and $TLG_{2.5}$ on PET images were measured using the volume viewer software. Each tumor was examined with a spherical-shaped volume of interest (VOI) that included the entire lesion in the axial, sagittal, and coronal planes. By using CT images, ^{18}F-FDG uptake of normal organs such as the bowel, stomach, and liver was not included in the VOI. SUV_{max} of the VOI was calculated as (decay-corrected activity/tissue volume)/(injected dose/body weight). $MTV_{2.5}$ was defined as total tumor volume with an SUV $\geq$ 2.5, and the $MTV_{2.5}$ and SUV_{mean} of the VOI were automatically calculated. $TLG_{2.5}$ was calculated as (mean SUV) × ($MTV_{2.5}$). In patients with SUV_{max} of < 2.5, $MTV_{2.5}$ and $TLG_{2.5}$ were not measured. In addition, clinical patterns of ^{18}F-FDG uptake in SPTs were categorized according to the proportion of ^{18}F-FDG uptake over the whole tumor volume (Hot-uptake: ≥70%, Mixed: 30%≤ <70%, and Defective type: <30%).

4. Case selection for gene expression of glucose metabolism in SPT

Each five SPTs, 5 pancreatic ductal adenocarcinomas (PCAs), and 5 non-neoplastic normal pancreatic tissue-samples were used in this study. The specimens were obtained from the archives of the Department of Pathology, Yonsei University, Seoul, Korea and from the Liver Cancer Specimen Bank of the National Research Resource Bank Program of the Korean Science and Engineering Foundation of the Ministry of Science and Technology. All tissues were collected as fresh snap-frozen samples immediately at the time of surgery. All carcinoma samples were comprised of more than 70% tumor cells, and none of the patients had received neo-adjuvant chemotherapy.

Authorization for the use of these tissues for research purposes was obtained from the Institutional Review Board of Yonsei University of College of Medicine.

5. RNA preparation

Total RNA was extracted using Trizol (Invitrogen Life Technologies, Carlsbad, CA, USA) according to the manufacturers' protocol. After DNase digestion and other clean-up procedures, RNA samples were quantified, aliquotted, and stored at -80℃ until use. For quality control, RNA purity and integrity were evaluated by denaturing gel electrophoresis, measurement of the A260/280 ratio, and analyzed using the 2100 bioanalyzer (Agilent Technologies, Santa Clara, CA, USA). For all samples, the RNA integrity number (RIN) scores were greater than 9.5.

6. Gene expression analysis

For DNA microarray hybridization, RNA was pooled by mixing equal amounts of total RNA. Biotin-labeled cRNA targets were synthesized starting from 1.5 μg of total RNA. Double-stranded cDNA synthesis was performed using the Illumina® TotalPrep RNA Amplification Kit (Illumina, San Diego, CA, USA), while biotin-UTP-labeled antisense RNA was transcribed *in vitr*o using Ambion's Kit (Ambion Life Technologies, Carlsbad, CA, USA). All steps of the labeling procedure were performed according to the manufacturers' protocol. Microarray experiments were conducted on the HumanHT-12 v4 Sentrix Expression BeadChip (Illumina). Hybridization of labeled cRNA to the BeadChip, washing, and scanning were performed according to the Illumina Bead Station 500´manual.

7. mRNA gene expression data preparation and statistical analysis

Raw data were extracted using the software provided by the manufacturer (Illumina Genome Studio v2011.1 (Gene Expression Module v1.9.0)). Expression intensities were normalized using quantile normalization techniques [35]. Using the normalized intensities, differentially expressed genes (DEGs) between non-neoplastic pancreatic tissue and pancreatic tumors (SPT, or PCA) were determined using the integrated statistical method previously reported[54]; 1) two independent tests were performed: Student's *t*-test and log2–median-ratio test; 2) adjusted *P*- values from each test were computed using an empirical distribution of the null hypothesis that the means of the genes were not different, which was obtained from random permutations of the samples; 3) the *P*- values from the two tests were combined to compute the overall *P* values using Stouffer's method[55], and 4) DEGs were selected as those with $P<0.01$ and a fold change >1.5. Finally, functional enrichment analysis of the DEGs was performed using DAVID software[56] to identify GOBPs and KEGG pathways represented by the genes in individual clusters with statistical significance

8. Western Blot

Whole lysates from tissue specimens were prepared using passive lysis buffer (Promega, Madison, WI, USA). Protein samples were separated by sodium dodecyl sulfate polyacrylamide gel electrophoresis and transferred to polyvinylidene difluoride membranes. Blots were blocked with Tris-buffered saline and Tween 20 containing 5 % skim milk, and incubated overnight at 4℃ with primary antibodies against GLUT1(Alpha Diagnostic, Cat. No. GT12-A), HK1 (Cell Signaling, Cat. No. 2024), ENO2 (antibodies-online, Cat. No. ABIN389272), PKM2 (Cell Signaling, Cat. No. 4053), LDHA (Cell Signaling, Cat. No. 3582), PDHA (Cell Signaling, Cat. No.3205). After washing, the membranes were incubated with the horseradish

peroxidase-conjugated secondary antibody (Santa Cruz Biotechnology, Inc., Santa Cruz, CA, USA) for 1 h at room temperature, washed, and developed with ECL-Plus (Amersham Pharmacia Biotech, Uppsala, Sweden).

9. Immunohistochemistry

Healthy available Paraffin-embedded tissue blocks of 36 patients were cut into 4-μm sections. Immunohistochemical analysis was performed using a Ventana XT automated stainer (Ventana Corporation, Tucson, AZ, USA) with antibodies against GLUT1(Alpha Diagnostic, Cat. No.GT12-A), HK1 (Cell Signaling, Cat. No. 2024), ENO2 (antibodies-online, Cat. No. ABIN389272), PKM2 (Cell Signaling, Cat. No. 4053), LDHA (Cell Signaling, Cat. No.3582), PDHA (Cell Signaling, Cat. No.3205), and Ki-67 (Dako, Cat. No. M7240).

10. Statistical Analysis

The continuous variables were expressed as mean± standard deviation and the categorical variables as frequency (%). ANOVA, Student t-test were used for comparative analysis and chi-square (Fisher's exact test, or linear-to-linear association if necessary) were used for correlating clinical pattern of FDG uptake and grade of immunohistochemistry for detecting glucose metabolism-related gene expression. Statistical analyses were performed using SPSS 20.0 for Windows (SPSS Inc., Chicago, IL, USA). *P*-values < 0.05 were considered to be statistically significant.

III. RESULTS

1. Clinical pattern of ^{18}F-FDG uptake in SPT of the pancreas

Thirty-six patients with SPTs took ^{18}FDG-PET scan for preoperative

evaluation. Thirty-five patients (97.2%) were female and only one was male with age, 34.8±11.2 years. Radiologic tumor size was 4.8±2.8 cm in maximum diameter. PET-related parameters were calculated in all SPTs. SUV_{max} was found to be 5.5±4.1 (g/cm^3), SUV_{mean} was 12.1±51.8 (g/cm^3), MTV2.5 was 31.5±59.6 (cm^3), and $TLG_{2.5}$ was 155.1±293.8 (g), respectively. Clinical pattern of ^{18}F-FDG uptake in SPT of the pancreas were classified according to proportion of ^{18}F-FDG uptake within the tumor. Hot-uptake type was identified in 19 patients (Figure 2-A, and B, 52.8%), mixed type in 5(Figure 2-C, and D, 13.8%), and defective type in 12 patients (Figure 2-E, and F, 33.4%).

When correlating the clinical patterns of ^{18}FDG-uptake with radiologic tumor size and PET-parameters, radiologic tumor size ($p=0.002$), SUV_{max} ($p=0,001$), SUV_{mean} ($p=0.037$), and $TLG_{2.5}$ ($p=0.013$) was significant different according to pattern of ^{18}F-FDG uptake in SPTs of the pancreas (ANOVA, $p<0.05$, Figure 3, and Supplementary 1). Mixed type of SPT was shown to be large in size with high intensity of ^{18}FDG uptake. It appeared that PET-based parameters of hot uptake type is higher than defective type of SPTs, however, there was no significant difference in radiologic tumor size and PET-based parameters between hot uptake and defective type (ANOVA, $p>0.05$).

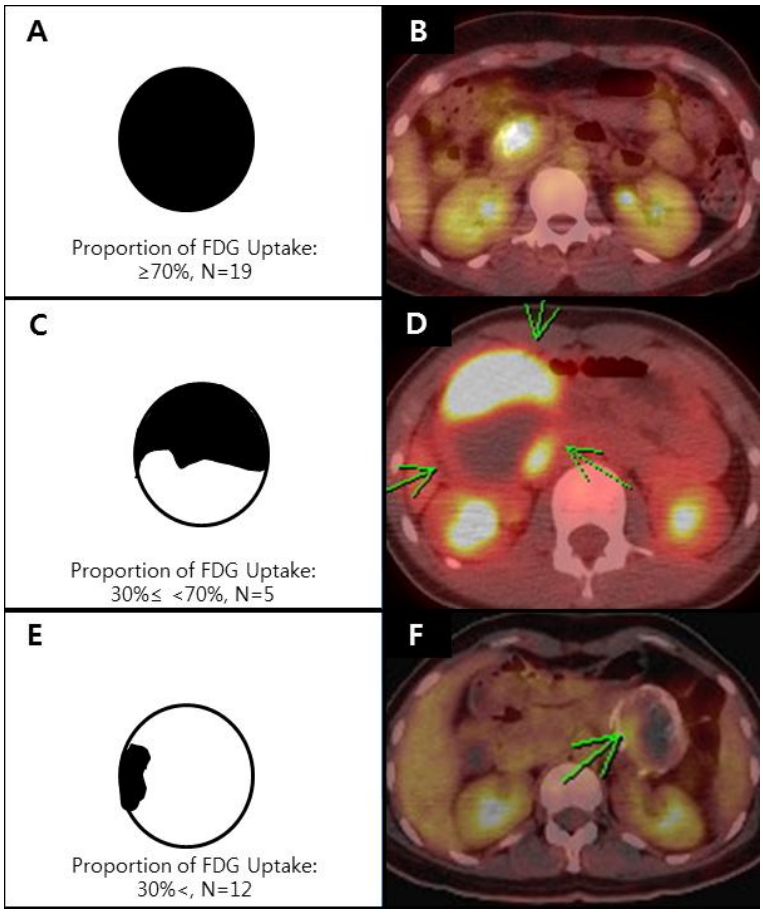

Figure 2 Clinical patterns of ^{18}FDG-uptake in SPT of the pancreas.

A: Hot-uptake type, B: Mixed type, and C: Defective type

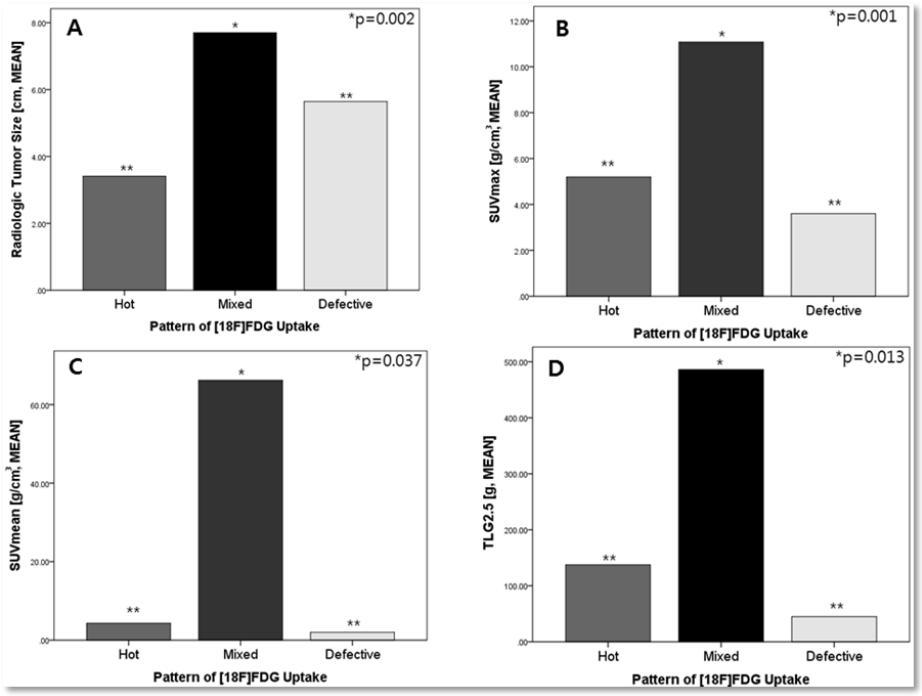

Figure 3 Differences in PET-based parameters according to pattern of ^{18}F-FDG uptake in SPT of the pancreas

*ANOVA, **p>0.05,

2. Gene expression profile for glucose metabolism in SPT of the pancreas

Typically, over-expression of β-catenin was noted in SPT comparing with PCA (fold change comparing normal pancreatic tissue in SPT, x4.3, $p=0.003$, and PCA, x1.6, $p>0.05$, Figure 4, and Supplementary II). Expression of GLUT-1 is significantly higher in PCA comparing to SPT of the pancreas (fold change comparing normal pancreatic tissue in SPT, x2.2, $0.01<p<0.05$, and PCA, x11.0, $p<0.01$). However, GLUT12, and GLUT-14 were noted to be highly expressed in SPT of the pancreas comparing with PCA ($p<0.01$). Glucose transporter, GLUT-6, was expressed in both SPT and PCA comparing to normal pancreatic tissue with marginal significance ($0.01<p<0.05$, Supplementary 2).

Hexokinases were also highly expressed in both SPT and PCA, but HK-I was strongly overexpressed in SPT of the pancreas comparing with PCA (SPT, x7.0, $p<0.01$ vs. PCA x3.7, $p<0.01$). To the contrary, expression of HK-2 in SPT was similar to normal pancreatic tissue (x1.9, $p>0.05$), but it was shown to be higher in PCA (x4.8, $p<0.01$). In addition, PFKM (phosphofructokinase), ENO2 (enolase-2), and PKM2 (pyruvate kinase) were also significantly overexpressed in SPT of the pancreas. To put all together, these data suggest that SPT has sufficient molecular apparatus for active glucose metabolism.

Interestingly, expression of PDHB (pyruvate dehydrogenase) was similar comparing to normal pancreatic tissue in both SPT (x1.0, $p>0.1$), and PCA (x -1.1, $p>0.1$), however, LDHA was noted to be significantly overexpressed in PCA comparing with normal pancreatic tissue (lactate dehydrogenase, x2.9, $p<0.01$), which is very contradictory to SPT in which there was decreased expression of LDHA, but similar to normal pancreatic tissue (x -1.1, $p>0.1$).

Figure 4 Summary of mRNA expression profile for glucose metabolism in SPT. SPTs showed increased gene expression for active glucose metabolism. Note that LDHA is highly expressed in PCA comparing to normal pancreatic tissue, but it slightly decreased in SPT without statistical significance (See also Supplementary II)

3. Protein expression for glucose metabolism in SPT of the pancreas

As shown in gene expression data, overexpression of HK1, PKM2, and ENO2 were also noted in protein level (Figure 5). Especially, expression of HK1 and ENO2 were apparently unique in SPT comparing to PCA. Overexpression of GLUT1 gene in SPT was noted with marginal significance (x 2.2, p=0.012) comparing with PCA (x11, p<0.001, Figure 4 and Supplementary II), however, GLUT1 expression in protein level was found to be similar between SPT and PCA. In particular, both expression of PDHB and LDHA in SPTs were observed similar to normal pancreatic tissue, but it was noted that LDHA was overexpressed in PCA as shown in gene expression data.

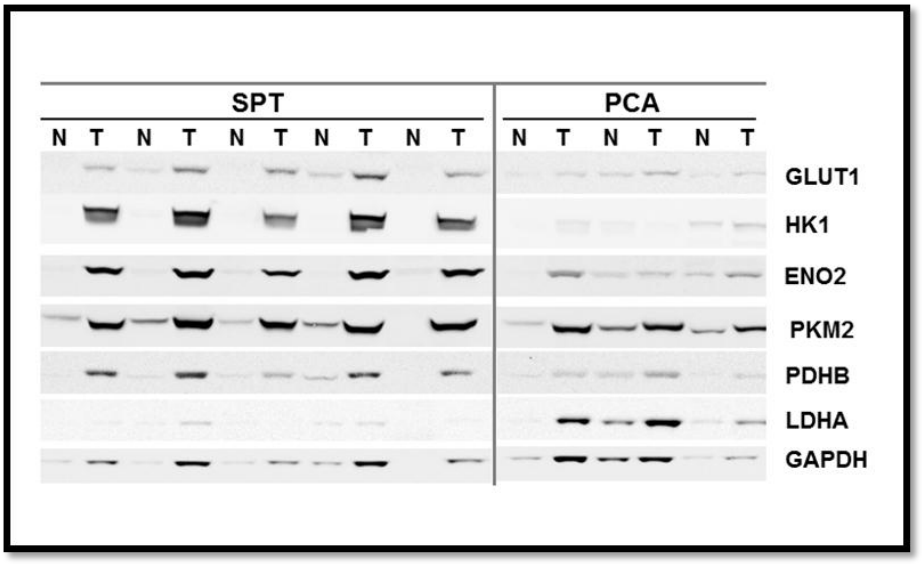

Figure 5 Glucose metabolism-related gene expressions in SPT of the pancreas (Western Blot)

4. Immunohistochemistry for glucose metabolism in SPT of the

pancreas

Most glucose metabolism-related genes found in gene-chip analysis were all confirmed in IHC of resected SPTs (Figure 6, and Table 1). GLUT-1 was found to be expressed in 31 patients (86.1%, Figure 6-A). Especially, over expression of ENO2 was noted comparing with normal acinar cells (Figure 6-C). LDHA and PDHB were also observed in all patients, which seemed similar or less to those in normal acinar cells (Figure 6-E, and F). HK-1 and PKM2 could not be assessed in 10 patients due to severe tumor cell necrosis. However, HK-1 was significantly expressed in all the rest 26 patients (Figure 6-B). PKM-2 was also clearly expressed in 20 patients (76.9%, Figure 6-D), but there was minimal expression (trance, ±) in 6 patients. All SPTs showed very low proliferative index (Figure 6-E, and F). Ki-67 expression less than 3% (range, 0-5%) was found in almost all patients (94.4%), and 23 SPTs (63.8%) showed Ki-67 expression was less than 1%.

Immunohistochemistry for identifying glucose metabolism-related genes was also performed in 5 patients with PCAs which were used as samples for gene expression (Supplementary 3). As expected, GLUT-1 was shown to be expressed in all 5 patients, however, HK1 was rarely expressed and no ENO2 expression was noted in PCAs. It was noted that PKM2, and LDHA was strongly expressed comparing to SPTs of the pancreas.

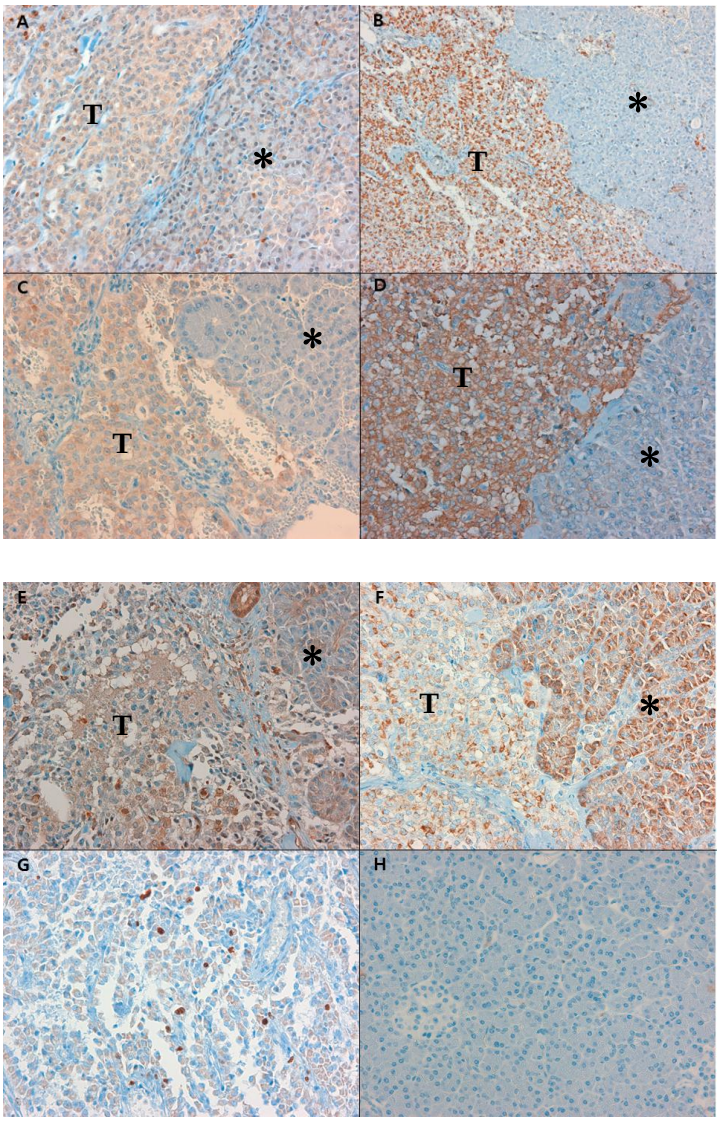

Figure 6 Expression of glucose metabolism related genes in immunohistochemistry. Expression of GLUT-1 (A), HK1 (B), ENO2 (C), PKM2 (D), LDHA (E), PDHD (F), and Ki-67 (in SPT, G, and normal acinar cells, H). Note that * indicates area of normal acinar cells, and T indicates tumor area of SPT.

Table 1 Immunohistochemistry of glucose-related genes in SPT of the pancreas

Patient Number	Gender	Age	Tumor Size (cm)	^{18}FDG-uptake pattern	GLUT-1	HK-1	ENO2	PKM2	Ki-67	Necrosis
1	Female	25	5.6	Hot	+	+	+	+/-	<1%	-
2	Female	46	5	Defective	-	++	+	+	<1%	-
3	Female	38	3.5	Mixed	+	++	+	N/A	<1%	+
4	Female	28	5	Defective	+	N/A	+	N/A	<1%	+
5	Female	28	6.8	Hot	+	N/A	+	N/A	<1%	+
6	Female	24	8.2	Hot	+	++	+	+	<1%	-
7	Female	32	1.7	Hot	+	++	+	+	1-2%	-
8	Female	25	4.9	Defective	+	++	+	+	1-2%	-
9	Female	31	5.3	Defective	+	N/A	+	N/A	0%	+
10	Female	46	6.5	Defective	+	N/A	+	N/A	0%	+
11	Female	45	2.3	Mixed	+	++	+	+	<1%	-
12	Female	12	10.1	Mixed	+	++	+	+	3%≤	-
13	Female	25	12.3	Hot	+	N/A	+	N/A	1-2%	+
14	Female	35	1.3	Hot	+	++	+	+	1-2%	-
15	Female	24	5.7	Hot	+	++	+	+	<1%	-
16	Female	62	1.5	Hot	+	++	+	+	<1%	-
17	Female	35	1.6	Mixed	+	++	+	+	<1%	-
18	Female	14	6.9	Hot	-	++	+	+/-	3%≤	-
19	Female	19	3.5	Mixed	-	++	+	+	1-2%	-
20	Female	47	4.2	Hot	+	++	+	+	<1%	-
21	Male	30	3.8	Hot	+	++	+	+	<1%	-
22	Female	48	1.5	Defective	+	++	+	+	<1%	-
23	Female	41	2.5	Defective	+	N/A	+	N/A	<1%	+
24	Female	38	6.5	Hot	+	N/A	+	N/A	<1%	+
25	Female	46	2	Defective	+	++	+	+	1-2%	-
26	Female	28	8	Defective	+	+	+	+/-	3%≤	-
27	Female	16	7	Hot	+	N/A	+	N/A	<1%	-
28	Female	45	3	-	-	N/A	+	+/-	<1%	+
29	Female	43	5.2	Defective	-	N/A	+	+/-	<1%	+
30	Female	22	8.5	Hot	+	+	+	+	1-2%	-
31	Female	40	8.3	Hot	+	++	+	+	1-2%	-
32	Female	35	1.6	Hot	+	++	+	+	<1%	-
33	Female	38	2	Hot	+	++	+	N/A	1-2%	-
34	Female	40	2.7	Hot	+	+	+	N/A	<1%	-
35	Female	42	1.5	Hot	+	++	+	+	1-2%	-
36	Female	23	5	Hot	+	++	+	+/-	<1%	-

N/A; not available due to necrosis

5. **Correlation between PET-based parameters and glucose metabolism-related gene expressions in SPT of the pancreas**

GLUT-1 expression was not associated with ^{18}FDG-uptake intensity in SPT. There was no difference in GLUT-1 expression according to the pattern of ^{18}FDG-uptake (p=0.646, Supplementary 4). However, expression of HK-I (p=0.014) and PKM2 (p=0.028) were found to be different according to the pattern of ^{18}FDG-uptake. Expression of HK-1 and PKM2 decreased in defective type comparing with hot+mixed type (Figure 7-A, and B). Intratumoral necrosis was associated with defective type of SPT (p=0.007, Figure 7-C). In addition, there was significant association between intratumoral necrosis and Ki-67 index (p=0.017, Table 2), indirectly suggesting SPT with intratumoral necrosis was related to toward lower Ki-67 index. Therefore, defective type had the tendency to show lower proliferation power comparing with Hot+ Mixed type of SPT (p=0.07, Figure 7-D). It was also observed SPT with high ^{18}F-FDG intensity (SUV_{max}) showed high Ki-67 index (ANOVA, p=0.002, Figure 8).

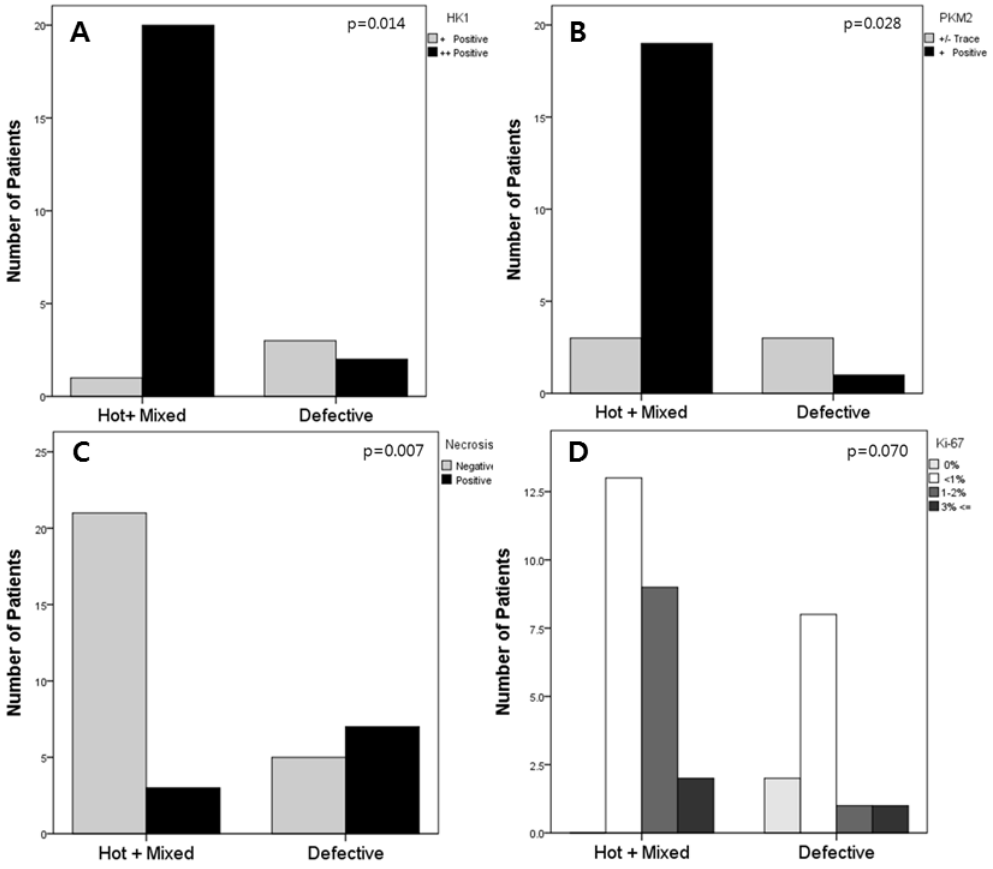

Figure 7 HK1, PKM2, Necrosis, and Ki-67 expression according to pattern of FDG-uptake

Table 2 Correlation between intratumoral necrosis and Ki-67 index

		Necrosis		P=value
		Negative	**Positive**	
Ki-67 (%)	0	0	2	0.017
	<1	14	7	
	1-2	9	1	
	3≤	3	0	

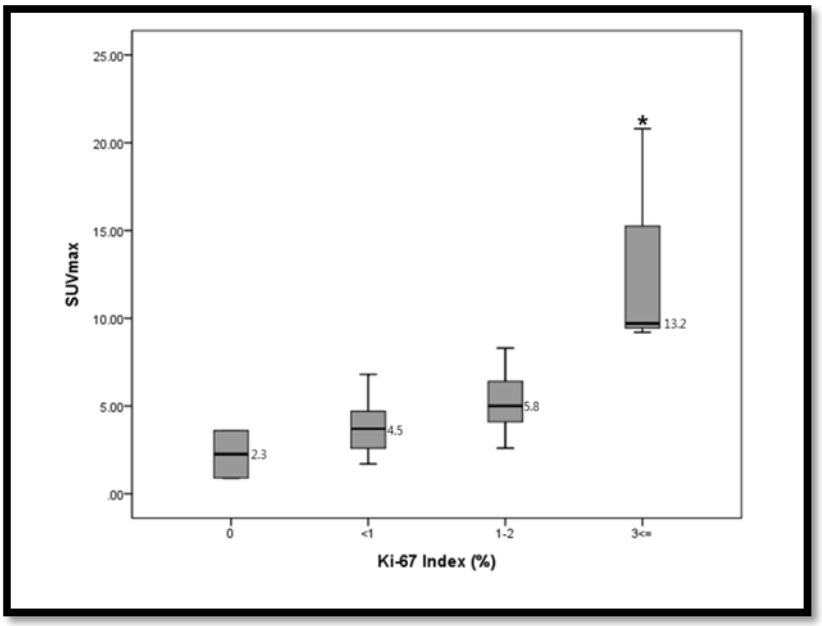

Figure 8 SUV_{max} values according to Ki-67 Index

*p=0.002, a number beside the box shows the mean value of SUV_{max}

6. Correlation between expressions of glucose metabolism related genes, pattern of FDG uptake and microscopic malignant feature of SPTs

Seven patients (19.4%) were found to have microscopic malignant features in resected SPTs. Microscopic malignant features included capsule invasion, perineural invasion, vascular invasion, infiltrative to pancreatic tissue, and peripancreatic tissue invasion. PET-based parameters, such as SUV_{max}, SUV_{mean}, $MTV_{2.5}$, and $TLG_{2.5}$ were similar between groups with microscopic benign and microscopic malignant features of SPTs ($p>0.05$, Table 3). There were no relationships between expression of GLUT-1, HK1, PKM2, Ki-67 index and microscopic malignant feature ($p>0.05$). However, defective type of SPTs were associated with benign-looking SPTs comparing with hot + mixed type of SPT, but did not reach the statistical significance ($p=0.070$, Table 4).

Table 3 Correlation between PET-based parameters and microscopic malignant features of SPTs

	Microscopic malignant features		P-value
	No (N=29)	Yes (N=7)	
SUV_{max}	5.1±4.0	6.9±4.5	0.299
SUV_{mean}	14.2±57.8	3.5±2.1	0.631
$MTV_{2.5}$	23.3±47.2	65.3±92.8	0.284
$TLG_{2.5}$	133.2±279.7	245.5±355.9	0.372
Tumor size	4.9±3.2	5.1±2.9	0.828

Table 4 Correlation between glucose metabolism-related gene expression and microscopic malignant features of SPTs

		Microscopic malignant features		**P-value**
		No (N=29)	Yes (N=7)	
GLUT-1	-	4	1	
	+	25	6	1.000
HK-1	+	3	1	
	++	17	5	1.000
PKM2	+/-	6	0	
	+	14	6	0.280
Necrosis	-	20	6	
	+	9	1	0.645
Ki-67	0	2	0	
	<1	15	6	
	1-2	10	-	
	3≤	2	1	0.781
Clinical pattern ^{18}FDG-uptake	Hot+Mixed	17	7	
	Defective	12	0	0.070

7. Literature review of available appearance of SPTs on ^{18}F-FDG-PET scan

There were few reports demonstrating available appearance of ^{18}F-FDG uptake of SPT on ^{18}F-FDG PET scan. Only 12 SPTs were found in 6 literatures. Hot-uptake type was noted in 6 patients and mixed in 3, and defective type in 3 patients. In spite of limited data, hot-uptake type and

mixed type of SPTs apparently harbored the characteristics of malignant behavior, such as microscopic malignant features, metastasis, and peritoneal seeding. Relatively high Ki-67 index was also noted in mixed type (Table 5).

Table 5 Literature reviews with available appearance of SPTs on ^{18}F-FDG FDG-PET scan

Case	Clinical Pattern ^{18}F-FDG uptake	Radiologic Tumor Size (cm)	SUV_{max}	Microscopic malignant features	Ki-67	Clinical behavior
16/F[50]	Hot	1.0	3.6	No	<1%	B
25/F[57]	Mixed	4.5	7.5	No	<5%	B
31/F[53]	Mixed	5.6	4.2	N/A	N/A	B
32/F	Defective	3.0	2.6	N/A	N/A	B
13/F[49]	Mixed	10.3	29.1	Yes	<5%	B
48/F	Defective	9.9	4.1	No	<1%	B
45/F	Hot	3.9	6.6	Yes	<1%	B
37/F	Hot	1.3	4.4	Yes	1%	B
16/M[58]	Hot	N/A	N/A	Yes (metastasis /seeding)	N/A	M
27/F[52]	Hot	2.6	12.8	N/A	N/A	B
37/F	Defective	1.6	2.2	N/A	N/A	B
*N/A	Hot	2 vs. 4	3.2 vs. 5.5	Yes metastasis/seeding	NA	M

*These tumors are all metastastic tumors to liver and peritoneum. Not available (N/A) information for primary pancreatic SPTs. B; benign behavior, M; malignant behavior

IV. DISCUSSION

To date, the investigation of SPT on ^{18}F-FDG PET or PET/CT is rarely

reported. According to literatures, intensity of ^{18}FDG-uptake in SPT was shown to be widely ranged. In some reports[35,59], SPT with mild or no ^{18}F-FDG uptake have been presented, and others reported SPT with intense ^{18}F-FGD uptake[49,50,53,58,60]. With accumulating clinical experiences of SPT, current application of PET scan to SPT of the pancreas is to test differentiating capacity of SPT from other malignant tumor, such as pancreatic cancer or neuroendocrine tumor [51,52,61] and clinical usefulness in staging as well as treatment planning[58,60]. Although several reports of high ^{18}F-FDG uptake in SPT were published, it is very rare to find a research to investigate the metabolomic mechanisms of SPT of the pancreas.

The exact mechanisms involved in glucose uptake of SPT are still unknown. In 2006, Sato, et al[53] reported two cases of SPT with increased accumulation of FDG uptake and tried to investigate the potential mechanism of ^{18}F-FDG uptake in SPT by performing immunohistochemistry. They showed poor expression of GLUT-1 and moderated expression of HK-II in SPTs, but it was not confirmative because of limited number of cases (only two cases). High cellular density of tumor cell[49] and cell density with abundant mitochondria[53] are currently available alternative mechanism to explain the intense FDG uptake in SPT of the pancreas.

In present study, we investigated the molecular mechanism of ^{18}F-FDG uptake in SPTs, and tried to correlate the metabolomics characteristics with clinical pattern of ^{18}F-FDG uptake in PET scan and microscopic malignant features of resected SPTs. To the best author's knowledge, the present study is thought to be the first report in dissecting molecular mechanism for glucose metabolism in SPT of the pancreas. According to our data, SPTs of the pancreas have increased molecular apparatus for glucose uptake and glycolysis to form pyruvate. It was found that GLUT-1, GLUT-6, GLUT-12, and GLUT-14 were largely expressed in SPT of the pancreas, and one of them, GLUT-1, known as principal glucose transporter in tumors, was generally expressed even in

protein level. In addition, enzymes involving glycolysis, such as HK1, ENO2, and PKM2 were also noted to be overexpressed, and they were all clearly confirmed by both western blot and immunohistochemistry. These molecular profiles are strongly suggesting that neoplastic cell of SPT of the pancreas basically possesses the increased capacity for glucose metabolism, which is exactly translated in appearance of SPT on ^{18}F-FDG -PET scan.

This study is also first one to try to categorize clinical pattern of ^{18}F-FDG uptake in SPTs; hot uptake, mixed, and defective type. This classification was based on the proportion of ^{18}F-FDG uptake within the whole tumor. Due to increased capacity of glucose metabolism, this pattern of ^{18}F-FDG uptake was different according to the amount of cystic and necrotic component in resected SPTs. SPT is very famous for frequent hemorrhage and necrosis within tumor. Cystic and necrotic area of tumor could not uptake ^{18}F-FDG. Dong, et al[49] recently showed viable tumor cellularity varied among tumors because of intratumoral hemorrhage, cystic change, and necrosis. They showed tumors with high cellularity showed strong ^{18}F-FDG uptake, whereas others with low cellularity resulting from extensive myxoid change or cystic change showed relatively lower FDG uptake, indicating that the degree of ^{18}F-FDG uptake in SPTs was correlated well to tumor cellularity. This observation was supported by our present data of immunohistochemistry. When correlating intratumoral necrosis with clinical pattern of ^{18}F-FDG uptake, defective type of SPTs was significantly related to intratumoral necrosis ($p=0.007$, Figure7-C). Therefore, present study is thought to provide the potential model to explain various (heterogeneous) pattern of ^{18}F-FDG -uptake in SPT of the pancreas.

In addition, intratumoral necrosis was associated with low Ki-67 index (Table 2) and defective type of SPT was related to intratumoral necrosis with toward lower Ki-67 index (Figure 7-C, and D). These observations indirectly suggesting that defective type of SPTs may be less likely to progress.

Defective type of SPT, resulted from intratumoral hemorrhagic necrosis due to weakened cell-to-cell adhesion[19], can cause chronic hypoxia and ischemic necrosis of viable solid portion of the tumor. If the tumors were not clinically detected even at this stage and or not treated immediately, totally necrotic tumor of the pancreas might be found. Recently, it was postulated marginally calcified *totally* necrotic pancreatic tumor might be a subset of SPT with near total necrosis[62] (may be defective type), and the present observation may support this hypothesis.

It is also interesting to note that clinical pattern of ^{18}F-FDG uptake in SPT apparently represents metabolic activity of SPT of the pancreas. Expression of HK-1 and PKM2 were closely correlated with pattern of ^{18}F-FDG uptake (Figure 7-A, B, and supplementary 4). It was observed that more frequent expression of HK-1 and PKM2 were noted in hot uptake and mixed type comparing to defective type. Especially, pyruvate kinase is the last rate-limiting enzyme in the glycolysis and catalyzes the conversion of phosphoenolpyruvate and ADP into pyruvate and ATP. PKM2 is known to be expressed predominantly in tumor cells and is important for cancer metabolism and tumor growth. Previous study showed that PKM2 expression was involved in early tumorigenesis[63] and increases in PKM2 levels were correlated with tumor size and stage[41]. Therefore, in early stage of SPTs (hot uptake, and mixed type; hot-uptake type with less hemorrhage or necrosis), PKM2 may place important role in tumorigenesis of SPTs. PKM2 exists as either a low-activity dimeric or high activity tetrameric form. The low activity of dimeric PKM2 promotes the conversion of pyruvate to lactate. In contrast, the high activity of tetrameric PKM2 promotes the conversion of pyruvate to acetyl-CoA and drives the tricarboxylic acid (TCA) cycle[43,64]. There have been several studies about PKM2 nuclear Translocation. Nuclear PKM2 has been shown to activate gene transcriptions and cell proliferation by co-operating β-catenin[65], STAT3[66], AND HIF-1/p300[67]. Nuclear PKM2 has

been reported to exist as a dimeric form, whereas cytoplasmic PKM2 exists as both dimeric and tetrameric form[66]. It is known that the tetramer to dimer ratio of PKM2 is not a fixed and oscillates depending on the presence of oncoproteins and one of the key metabolic intermediates, fructose-1,6-biphosphate[68], which is converted from fructose-6-phosphate by aid of phosphofructokinase (Figure 1). Our mRNA expression data clearly showed that high expression of PFK (more than 5 times, $p<0.001$, Figure 2 and Supplementary 2). Therefore, it is thought that high level of fructose-1,6-biphosphate in SPTs could keep PKM2 high-active tetrameric form. In fact, it was observed nearly all PKM2 of SPT was found in cytoplasm with sparing nucleus in immunohistochemistry (Figure 6-D). To the contrary, considering expression of LDHA was predominant in PCA (Figure 4, 5, Supplementary 2, and 3) and biologic behavior of PCA [high Ki-67 index] is generally much aggressive comparing with SPTs, PKM2 in PCA may be low-activity dimeric form. However, it was difficult to confirm additional nuclear location of PKM2 in PCA because there was too strong cytoplasmic staining of PKM2 in PCA, playing as background noise in interpretation (Data not shown). In spite of similar capacity of ^{18}F-FDG uptake in both SPTs and PCA, this metabolomics differences may differentiate biologic behavior of these two tumors in clinical oncology.

HK catalyzes the conversion of glucose to glucose-6-phosphate, the first and rate-limiting step in the glycolytic pathway. HK1 is known to be either free in the cytosol or bound to the outside of the outer mitochondrial membrane. The proportion of HK1 bound to the mitochondria is tissue specific, and varies with the metabolic state of the cell. Binding of HK1 to the outer mitochondrial membrane is thought to induce a conformational change that renders the enzyme less sensitive to inhibition by its product, increasing glucose phosphorylation, and preventing tumor apoptosis[69,70 71]. Usually, HK2 is regarded as principle enzyme in cancer metabolism, but our study suggests

that HK1 was main enzyme converting glucose to glucose-6-phosphate in SPT of the pancreas. Exact role of HK1 and PKM2 in tumorigenesis of SPT remains to be investigated further.

It was also found that SPT with high Ki-67 index was related to high SUV_{max} (Figure 8). Considering tumor size and PET-related parameters, such as SUV_{max}, SUV_{mean}, and $TLG_{2.5}$ were larger and higher in mixed type of SPTs (Figure 1 and Supplementary I), mixed type of SPT in FDG uptake may be biologically active form of tumor with highest Ki-67 index. Due to limited number of mixed type in our data set (n=5 patients), it is difficult to exactly confirm this potential relationship, but this observation is thought to be very important because Ki 67 index and tumor proliferation are previously reported to associated with aggressive biological behavior of SPT of the pancreas. Tang, et al[33] reported 2 cases with clinically aggressive SPT with high mitotic rate, 70/50 high power field(HPF) and 35/50 HPF, respectively, comparing with SPT pursuing indolent clinical course (mean 1.1/50 HPF). Hibi, et al [72] also reported a case with aggressive SPT with multiple metastases, leading to tumor-related mortality 8 years after initial presentation. They evaluated quantitative Ki-67 index and demonstrated a significant increase of up to 35% of Ki-67 index as the disease progressed. Lai et al [73] performed cytometric analysis of cellular DNA content, suggesting high DNA index and aneuploidy folow cytometry results are considered a poorer prognosis. Therefore, clinically, it can be recommended that SPT with high SUV_{max} (for example, hot uptake and mixed type) should be aggressively treated from the metabolomics point of view, because PET-based parameter, especially high SUV_{max} was related to increased Ki-67 index. In addition, small hot-uptake type of SPT should be considered for resection because it is difficult to differentiate from other malignant tumors of the pancreas, such as pancreatic cancer, and neuroendocrine tumor, when the tumor did not show typical radiologic characteristics of SPT of the pancreas[52,61]. On the other hand,

defective type of SPTs was associated with low expression of HK1/PKM2, intratumoral necrosis, and tended to have lower proliferation with low metabolic capacity (Figure 3), suggesting this type of tumor might be less progressive and would follow indolent clinical course. Considering most patients with SPTs are young female patients with active social activity, surgery for SPTs with defective type of ^{18}F-FDG uptake could be reserved according to patient's social activity, and physical conditions, because it cannot be denied that pancreatectomy is related to high rate of postoperative morbidity with potential mortality in spite of improved perioperative management[74] (Figure 9).

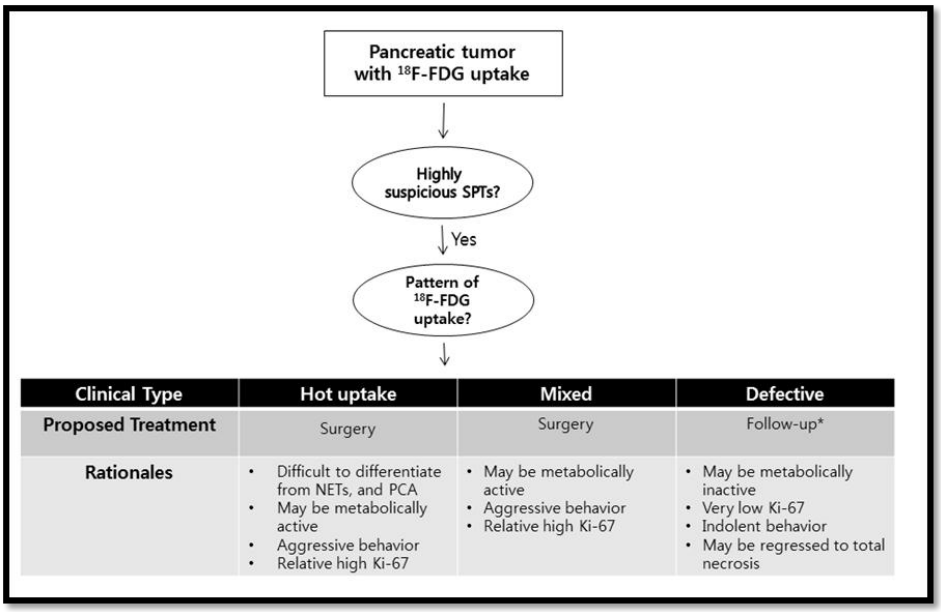

Clinical Type	Hot uptake	Mixed	Defective
Proposed Treatment	Surgery	Surgery	Follow-up*
Rationales	• Difficult to differentiate from NETs, and PCA • May be metabolically active • Aggressive behavior • Relative high Ki-67	• May be metabolically active • Aggressive behavior • Relative high Ki-67	• May be metabolically inactive • Very low Ki-67 • Indolent behavior • May be regressed to total necrosis

Figure 9 Proposing surgical strategy for SPTs of the pancreas based on the pattern of ^{18}F-FDG uptake

Nakagohri, et al[59] recently reported most SPTs (5 out of 6 tumors) showed strong accumulation of FDG on PET scan, showing SPTs with high FDG uptake were related to microscopic venous and perineural invasion. Conversely, the tumors without intense FDG uptake had neither microscopic venous invasion nor nerve invasion, suggesting potential relationship between the SUV and histological malignancy. In our present data, it was observed that there was no relationship between malignant microscopic feature of resected SPT and GLUT-1, HK1, intratumoral necrosis, and Ki-67 index. However, pattern of ^{18}F-FDG uptake of SPT was shown to be related to microscopic malignant features of SPT with marginal significance (p=0.070, Table 7). Although, it is known that any histopathologic features are not predictable for clinical behavior of malignancy, recurrence and metastasis[32,33,37], Estrella, et a[75] recently suggested the importance of pathologic evaluation in risk assessment in patients with SPTs by showing muscular vessel invasion, tumor T stage by European Neuroendocrine Tumors Society (ENETS) classification[76], ENETS stage grouping, and stage grouping by the American Joint Committee on Cancer[77] were significant predictors of disease-specific survival in SPTs. Therefore, further studies based on large number of patients with SPTs need to be investigated to unveil potential relationship of histological malignant feature of SPT and intensity of FDG uptake to predict biological tumor behavior. It would be also interesting to investigate the metabolomics differences between indolent type of SPTs and those with clinically aggressive behavior based on current observation. What makes indolent SPTs change into aggressive biologic behavior? What differences would exist between two types of SPTs from the view point of metabolism? Why should SPT increase glucose metabolism in spite of low-proliferation? Future studies based on basic and clinical research will provide us with the right answers to this *surgical egnigma,* pancreatic SPTs.

V. CONCLUSION

This study is the first investigation to dissect metabolomic characteristics in SPT of the pancreas. SPTs basically possessed active molecular capacity for increasing glucose metabolism, explaining well why SPT of the pancreas are well visualized in ^{18}F-FDG-PET scan. Clinical patterns of FDG were determined according to amount of intratumoral hemorrhagic necrosis and can be classified into three types; hot uptake, mixed, and defective type. Defective type of SPTs was associated with low metabolic activity and apparently related to low Ki-67 index, suggesting surgery can be reserved in this type of SPTs. Based on large volume-materials, characterization of metabolomics differences between indolent and aggressive SPTs will be the next future study to unveil *surgical enigma*, SPT of the pancreas.

VI. REFERENCES

1. Yoon WJ, Lee JK, Lee KH, Ryu JK, Kim YT, Yoon YB. Cystic neoplasms of the exocrine pancreas: an update of a nationwide survey in Korea. Pancreas 2008;37:254-8.
2. VK F. Tumor of the pancreas. In Atlas of tumor pathology. Armed Forces Institute of Pathology. Washington DC, .
3. Hamoudi AB, Misugi K, Grosfeld JL, Reiner CB. Papillary epithelial neoplasm of pancreas in a child. Report of a case with electron microscopy. Cancer 1970;26:1126-34.
4. Wilson MB, Adams DB, Garen PD, Gansler TS. Aspiration cytologic, ultrastructural, and DNA cytometric findings of solid and papillary tumor of the pancreas. Cancer 1992;69:2235-43.
5. Ferlan-Marolt V, Pleskovic L, Pegan V. Solid papillary-cystic tumor of the pancreas. Hepatogastroenterology 1999;46:2978-82.
6. Nishihara K, Nagoshi M, Tsuneyoshi M, Yamaguchi K, Hayashi I. Papillary cystic tumors of the pancreas. Assessment of their malignant potential. Cancer 1993;71:82-92.
7. Saiura A, Umekita N, Matsui Y, Maeshiro T, Miyamoto S, Kitamura M, et al. Successful surgical resection of solid cystic tumor of the pancreas with multiple liver metastases and a tumor thrombus in the portal vein. Hepatogastroenterology 2000;47:887-9.
8. Ky A, Shilyansky J, Gerstle J, Taylor G, Filler RM, Grace N, et al. Experience with papillary and solid epithelial neoplasms of the pancreas in children. J Pediatr Surg 1998;33:42-4.
9. Kloppel G SE LD. Histological Typing of Tumor of the Exocrine Pancreas. New York, Springer.
10. Papavramidis T, Papavramidis S. Solid pseudopapillary tumors of the pancreas: review of 718 patients reported in English literature. J Am Coll

Surg 2005;200:965-72.
11. Sperti C, Berselli M, Pasquali C, Pastorelli D, Pedrazzoli S. Aggressive behaviour of solid-pseudopapillary tumor of the pancreas in adults: a case report and review of the literature. World J Gastroenterol 2008;14:960-5.
12. Takahashi Y, Fukusato T, Aita K, Toida S, Fukushima J, Imamura T, et al. Solid pseudopapillary tumor of the pancreas with metastases to the lung and liver. Pathol Int 2005;55:792-6.
13. Zinner MJ, Shurbaji MS, Cameron JL. Solid and papillary epithelial neoplasms of the pancreas. Surgery 1990;108:475-80.
14. Abraham SC, Klimstra DS, Wilentz RE, Yeo CJ, Conlon K, Brennan M, et al. Solid-pseudopapillary tumors of the pancreas are genetically distinct from pancreatic ductal adenocarcinomas and almost always harbor beta-catenin mutations. Am J Pathol 2002;160:1361-9.
15. Tanaka Y, Kato K, Notohara K, Hojo H, Ijiri R, Miyake T, et al. Frequent beta-catenin mutation and cytoplasmic/nuclear accumulation in pancreatic solid-pseudopapillary neoplasm. Cancer Res 2001;61:8401-4.
16. Polakis P. Wnt signaling and cancer. Genes Dev 2000;14:1837-51.
17. Satoh S, Daigo Y, Furukawa Y, Kato T, Miwa N, Nishiwaki T, et al. AXIN1 mutations in hepatocellular carcinomas, and growth suppression in cancer cells by virus-mediated transfer of AXIN1. Nat Genet 2000;24:245-50.
18. Munemitsu S, Albert I, Souza B, Rubinfeld B, Polakis P. Regulation of intracellular beta-catenin levels by the adenomatous polyposis coli (APC) tumor-suppressor protein. Proc Natl Acad Sci U S A 1995;92:3046-50.
19. Kang CM, Kim HK, Kim H, Choi GH, Kim KS, Choi JS, et al. Expression of Wnt target genes in solid pseudopapillary tumor of the pancreas: a pilot study. Pancreas 2009;38:e53-9.
20. Crawford HC, Fingleton BM, Rudolph-Owen LA, Goss KJ, Rubinfeld B, Polakis P, et al. The metalloproteinase matrilysin is a target of beta-catenin

transactivation in intestinal tumors. Oncogene 1999;18:2883-91.

21. Shtutman M, Zhurinsky J, Simcha I, Albanese C, D'Amico M, Pestell R, et al. The cyclin D1 gene is a target of the beta-catenin/LEF-1 pathway. Proc Natl Acad Sci U S A 1999;96:5522-7.
22. He TC, Sparks AB, Rago C, Hermeking H, Zawel L, da Costa LT, et al. Identification of c-MYC as a target of the APC pathway. Science 1998;281:1509-12.
23. Min Kim S, Sun CD, Park KC, Kim HG, Lee WJ, Choi SH. Accumulation of beta-catenin protein, mutations in exon-3 of the beta-catenin gene and a loss of heterozygosity of 5q22 in solid pseudopapillary tumor of the pancreas. J Surg Oncol 2006;94:418-25.
24. Lieber MR, Lack EE, Roberts JR, Jr., Merino MJ, Patterson K, Restrepo C, et al. Solid and papillary epithelial neoplasm of the pancreas. An ultrastructural and immunocytochemical study of six cases. Am J Surg Pathol 1987;11:85-93.
25. Kallichanda N, Tsai S, Stabile BE, Buslon V, Delgado DL, French SW. Histogenesis of solid pseudopapillary tumor of the pancreas: the case for the centroacinar cell of origin. Exp Mol Pathol 2006;81:101-7.
26. Schlosnagle DC, Campbell WG, Jr. The papillary and solid neoplasm of the pancreas: a report of two cases with electron microscopy, one containing neurosecretory granules. Cancer 1981;47:2603-10.
27. Yagihashi S, Sato I, Kaimori M, Matsumoto J, Nagai K. Papillary and cystic tumor of the pancreas. Two cases indistinguishable from islet cell tumor. Cancer 1988;61:1241-7.
28. Matsunou H, Konishi F. Papillary-cystic neoplasm of the pancreas. A clinicopathologic study concerning the tumor aging and malignancy of nine cases. Cancer 1990;65:283-91.
29. Miettinen M, Partanen S, Fraki O, Kivilaakso E. Papillary cystic tumor of the pancreas. An analysis of cellular differentiation by electron microscopy

and immunohistochemistry. Am J Surg Pathol 1987;11:855-65.

30. Chen C, Jing W, Gulati P, Vargas H, French SW. Melanocytic differentiation in a solid pseudopapillary tumor of the pancreas. J Gastroenterol 2004;39:579-83.

31. Geers C, Moulin P, Gigot JF, Weynand B, Deprez P, Rahier J, et al. Solid and pseudopapillary tumor of the pancreas--review and new insights into pathogenesis. Am J Surg Pathol 2006;30:1243-9.

32. Martin RC, Klimstra DS, Brennan MF, Conlon KC. Solid-pseudopapillary tumor of the pancreas: a surgical enigma? Ann Surg Oncol 2002;9:35-40.

33. Tang LH, Aydin H, Brennan MF, Klimstra DS. Clinically aggressive solid pseudopapillary tumors of the pancreas: a report of two cases with components of undifferentiated carcinoma and a comparative clinicopathologic analysis of 34 conventional cases. Am J Surg Pathol 2005;29:512-9.

34. Canzonieri V, Berretta M, Buonadonna A, Libra M, Vasquez E, Barbagallo E, et al. Solid pseudopapillary tumour of the pancreas. Lancet Oncol 2003;4:255-6.

35. Kang CM, Kim KS, Choi JS, Kim H, Lee WJ, Kim BR. Solid pseudopapillary tumor of the pancreas suggesting malignant potential. Pancreas 2006;32:276-80.

36. Sclafani LM, Reuter VE, Coit DG, Brennan MF. The malignant nature of papillary and cystic neoplasm of the pancreas. Cancer 1991;68:153-8.

37. Kim CW, Han DJ, Kim J, Kim YH, Park JB, Kim SC. Solid pseudopapillary tumor of the pancreas: can malignancy be predicted? Surgery 2011;149:625-34.

38. Chakhachiro ZI, Zaatari G. Solid-pseudopapillary neoplasm: a pancreatic enigma. Arch Pathol Lab Med 2009;133:1989-93.

39. J AC, Lozano MD, Rotellar F, Marti P, Pedano N, Arredondo J, et al. Solid pseudopapillary tumor of the pancreas (SPPT). Still an unsolved enigma.

Rev Esp Enferm Dig 2010;102:722-8.
40. Koppenol WH, Bounds PL, Dang CV. Otto Warburg's contributions to current concepts of cancer metabolism. Nat Rev Cancer 2011;11:325-37.
41. Mazurek S, Boschek CB, Hugo F, Eigenbrodt E. Pyruvate kinase type M2 and its role in tumor growth and spreading. Semin Cancer Biol 2005;15:300-8.
42. Mazurek S. Pyruvate kinase type M2: a key regulator of the metabolic budget system in tumor cells. Int J Biochem Cell Biol 2011;43:969-80.
43. Vander Heiden MG, Cantley LC, Thompson CB. Understanding the Warburg effect: the metabolic requirements of cell proliferation. Science 2009;324:1029-33.
44. Smith TA. The rate-limiting step for tumor [18F]fluoro-2-deoxy-D-glucose (FDG) incorporation. Nucl Med Biol 2001;28:1-4.
45. Avril N. GLUT1 expression in tissue and (18)F-FDG uptake. J Nucl Med 2004;45:930-2.
46. Lodge MA, Lucas JD, Marsden PK, Cronin BF, O'Doherty MJ, Smith MA. A PET study of 18FDG uptake in soft tissue masses. Eur J Nucl Med 1999;26:22-30.
47. Nakamoto Y, Higashi T, Sakahara H, Tamaki N, Kogire M, Doi R, et al. Delayed (18)F-fluoro-2-deoxy-D-glucose positron emission tomography scan for differentiation between malignant and benign lesions in the pancreas. Cancer 2000;89:2547-54.
48. Shimoda W, Hayashi M, Murakami K, Oyama T, Sunagawa M. The relationship between FDG uptake in PET scans and biological behavior in breast cancer. Breast Cancer 2007;14:260-8.
49. Dong A, Wang Y, Dong H, Zhang J, Cheng C, Zuo C. FDG PET/CT findings of solid pseudopapillary tumor of the pancreas with CT and MRI correlation. Clin Nucl Med 2013;38:e118-24.

50. Shimada K, Nakamoto Y, Isoda H, Maetani Y, Yamashita R, Arizono S, et al. F-18 fluorodeoxyglucose uptake in a solid pseudopapillary tumor of the pancreas mimicking malignancy. Clin Nucl Med 2008;33:766-8.
51. Guan ZW, Xu BX, Wang RM, Sun L, Tian JH. Hyperaccumulation of (18)F-FDG in order to differentiate solid pseudopapillary tumors from adenocarcinomas and from neuroendocrine pancreatic tumors and review of the literature. Hell J Nucl Med 2013;16:97-102.
52. Kim YI, Kim SK, Paeng JC, Lee HY. Comparison of F-18-FDG PET/CT findings between pancreatic solid pseudopapillary tumor and pancreatic ductal adenocarcinoma. Eur J Radiol 2014;83:231-5.
53. Sato M, Takasaka I, Okumura T, Shioyama Y, Kawasaki H, Mise Y, et al. High F-18 fluorodeoxyglucose accumulation in solid pseudo-papillary tumors of the pancreas. Ann Nucl Med 2006;20:431-6.
54. Paterson EL, Kolesnikoff N, Gregory PA, Bert AG, Khew-Goodall Y, Goodall GJ. The microRNA-200 family regulates epithelial to mesenchymal transition. ScientificWorldJournal 2008;8:901-4.
55. Wang B, Herman-Edelstein M, Koh P, Burns W, Jandeleit-Dahm K, Watson A, et al. E-cadherin expression is regulated by miR-192/215 by a mechanism that is independent of the profibrotic effects of transforming growth factor-beta. Diabetes 2010;59:1794-802.
56. Bolos V, Grego-Bessa J, de la Pompa JL. Notch signaling in development and cancer. Endocr Rev 2007;28:339-63.
57. Guan ZW, Sun L, Wang YQ, Xu BX. Solid pseudopapillary tumor of the pancreas and concomitant urogenital malformations in a young woman. Diagn Pathol 2013;8:35.
58. Treglia G, Caporale N, Rufini V, Callea F, Locatelli F, Giordano A. Usefulness of 18F-FDG PET/CT in an unusual case of solid-pseudopapillary pancreatic tumor in childhood with aggressive behavior. Clin Nucl Med 2013;38:e35-7.

59. Nakagohri T, Kinoshita T, Konishi M, Takahashi S, Gotohda N. Surgical outcome of solid pseudopapillary tumor of the pancreas. J Hepatobiliary Pancreat Surg 2008;15:318-21.
60. Lee JK, Tyan YS. Detection of a solid pseudopapillary tumor of the pancreas with F-18 FDG positron emission tomography. Clin Nucl Med 2005;30:187-8.
61. Dong A, Dong H, Zhang L, Zuo C. Hypermetabolic lesions of the pancreas on FDG PET/CT. Clin Nucl Med 2013;38:e354-66.
62. Kang CM, Hwang HK, Kim H, Kim H, Chung YE, Park JS, et al. Marginally calcified totally necrotic tumor of the pancreas: a subset of solid pseudopapillary tumor with near-total necrosis? Pancreas 2013;42:184-6.
63. Wittwer JA, Robbins D, Wang F, Codarin S, Shen X, Kevil CG, et al. Enhancing mitochondrial respiration suppresses tumor promoter TPA-induced PKM2 expression and cell transformation in skin epidermal JB6 cells. Cancer Prev Res (Phila) 2011;4:1476-84.
64. Christofk HR, Vander Heiden MG, Harris MH, Ramanathan A, Gerszten RE, Wei R, et al. The M2 splice isoform of pyruvate kinase is important for cancer metabolism and tumour growth. Nature 2008;452:230-3.
65. Yang W, Xia Y, Ji H, Zheng Y, Liang J, Huang W, et al. Nuclear PKM2 regulates beta-catenin transactivation upon EGFR activation. Nature 2011;480:118-22.
66. Gao X, Wang H, Yang JJ, Liu X, Liu ZR. Pyruvate kinase M2 regulates gene transcription by acting as a protein kinase. Mol Cell 2012;45:598-609.
67. Luo W, Hu H, Chang R, Zhong J, Knabel M, O'Meally R, et al. Pyruvate kinase M2 is a PHD3-stimulated coactivator for hypoxia-inducible factor 1. Cell 2011;145:732-44.
68. Ashizawa K, Willingham MC, Liang CM, Cheng SY. In vivo regulation of monomer-tetramer conversion of pyruvate kinase subtype M2 by glucose is mediated via fructose 1,6-bisphosphate. J Biol Chem 1991;266:16842-6.

69. Mathupala SP, Ko YH, Pedersen PL. Hexokinase II: cancer's double-edged sword acting as both facilitator and gatekeeper of malignancy when bound to mitochondria. Oncogene 2006;25:4777-86.
70. Gelb BD, Adams V, Jones SN, Griffin LD, MacGregor GR, McCabe ER. Targeting of hexokinase 1 to liver and hepatoma mitochondria. Proc Natl Acad Sci U S A 1992;89:202-6.
71. Robey RB, Hay N. Mitochondrial hexokinases, novel mediators of the antiapoptotic effects of growth factors and Akt. Oncogene 2006;25:4683-96.
72. Hibi T, Ojima H, Sakamoto Y, Kosuge T, Shimada K, Sano T, et al. A solid pseudopapillary tumor arising from the greater omentum followed by multiple metastases with increasing malignant potential. J Gastroenterol 2006;41:276-81.
73. Lai HW, Su CH, Li AF, Wu LH, Shyr YM, Chen TH, et al. Malignant solid and pseudopapillary tumor of the pancreas--clinicohistological, immunohistochemical, and flow cytometric evaluation. Hepatogastroenterology 2006;53:291-5.
74. Mezhir JJ. Management of complications following pancreatic resection: an evidence-based approach. J Surg Oncol 2013;107:58-66.
75. Estrella JS, Li L, Rashid A, Wang H, Katz MH, Fleming JB, et al. Solid pseudopapillary neoplasm of the pancreas: clinicopathologic and survival analyses of 64 cases from a single institution. Am J Surg Pathol 2014;38:147-57.
76. Rindi G, Kloppel G, Alhman H, Caplin M, Couvelard A, de Herder WW, et al. TNM staging of foregut (neuro)endocrine tumors: a consensus proposal including a grading system. Virchows Arch 2006;449:395-401.
77. SB E. American Joint Committee on Cancer, AJCC Cancer Staging Manual. New York: Springer. 2010.

Supplementary 1 Correlation between pattern of ^{18}FDG uptake and radiologic PET-parameters

Type	Proportion of ^{18}FDG uptake	Age (years)	Radiologic Tumor Size	SUV_{max} (g/cm^3)	SUV_{mean} (g/cm^3)	$MTV_{2.5}$ (cm^3)	$TLG_{2.5}$(g)
Hot (n=19)	70%≤	36.3±10.8[a]	3.4±2.2[a]	5.2±2.8[a]	4.3±5.3[a]	34.4±69.9[a]	137.6±286.2[a]
Mixed (n=5)	30≤ <70%	25.2±13.9[a]	8.4±3.6[b]	11.1±7.1[b]	66.2±138.3[b]	55.7±64.4[a]	485.9±438.8[b]
Defective (n=12)	<30%	33.4±9.8[a]	5.6±2.0[a]	3.6±2.3[a]	2.0±1.5 [a]	16.8±35.7[a]	44.8±84.1[a]
p-value		0.146	0.002	0.001	0.037	0.462	0.013

[1]Statistical significances were tested by one-way analysis of variances (ANOVA) among groups. [2]The same letters (a, or b) in same column indicate non-significant differences between groups based on Turkey's multiple comparison test

Supplementary 2 Glucose metabolism-related gene expression in SPT and PCA (gene-chip analysis)

Gene Name	**Gene ID**	**Gene Description [*Homo sapiens* (human)]**	**Fold change comparing to normal pancreatic tissue**			
			SPT	p-value	**PCA**	p-value
CTNNB1	3091	catenin (cadherin-associated protein), beta 1, 88kDa	4.38437	0.003	1.698453	0.398
SLC2A1 [GLUT1]	6513	solute carrier family 2 (facilitated glucose transporter), member 1	2.217704146	0.012	11.0109781	<0.001
SLC2A6 [GLUT6]	11182	solute carrier family 2 (facilitated glucose transporter), member 6	2.466678738	0.031	2.120729135	0.035
SLC2A12 [GLUT12]	154091	solute carrier family 2 (facilitated glucose transporter), member 13,	19.81899308	<0.001	2.128288681	0.067
SLC2A14 [GLUT14]	144195	solute carrier family 2 (facilitated glucose transporter), member 14	2.600510327	0.008	2.54506771	0.027
HK1	3098	hexokinase 1	7.011942609	<0.001	3.722430211	0.006
HK2	3099	hexokinase 2	1.97208179	0.384	4.868928656	0.002
HK3	3101	hexokinase 3	-1.091921079	0.915	1.275390409	0.37
PFKM	5213	phosphofructokinase, muscle	5.35062582	<0.001	3.682860976	0.001
ENO1	2023	Enolase 1	-1.124513644	0.921	2.608696046	<0.001
ENO2	2026	Enolase 2	21.11439687	<0.001	9.02228159	<0.001
ENO3	2027	Enolase 3	1.560983176	0.085	1.344360654	0.372
PKM2	5315	pyruvate kinase, muscle	6.282950108	<0.001	3.682860976	0.001
PDHB	5162	pyruvate dehydrogenase (lipoamide) beta	1.095231811	0.852	-1.136414128	0.370
LDHA	3939	lactate dehydrogenase A	-1.130851243	2.968	0.966789424	0.003

Supplementary 3 Immunohistochemistry of glucose metabolism-related genes in 5 PCA samples

Sample Number	GLUT-1	HK-I	ENO2	PKM2	PDHB	LDHA	Ki-67
1	+	+	-	+++	+	++	30%
2	+	-	-	+++	+	++	8%
3	-	-	-	+++	+	++	20%
4	+	-	-	++	+	++	30%
5	+	-	-	++	+	++	30%

PCA; pancreatic ductal adenocarcinoma

Supplementary 4 Correlation between glucose metabolomics and pattern of ^{18}FDG-uptake pattern in SPTs

		Clinical pattern of ^{18}FDG-uptake		
		Hot+ Mixed	**Defective**	**P-value**
GLUT-1	-	4	1	
	+	20	11	0.646
HK-1	+	1	3	
	++	20	2	0.014
PKM2	+/-	3	3	
	+	19	1	0.028
Necrosis	-	21	5	
	+	3	7	0.007
Ki-67	0	0	2	
	<1	13	8	
	1-2	9	1	
	3≤	2	1	0.070

ABSTRACT (IN KOREAN)

췌장의 고형성가성유두상종양에서 대사관련 유전자 분석을 통한 ^{18}F-FDG PET-scan에서의 고강도 신호와의 관계성 규명

< 지도교수: 이 우 정 >

연세대학교 대학원 의학과

강 창 무

배경: 췌장에서 발생하는 고형성가성유두상종양은 매우 드문 췌장병리로서 절대적으로 여자에서 많이 발생한다. 완전한 수술적 절제가 치료의 원칙이지만, 아직까지 이 종양의 기원이나 자연경과에 대해서는 확실히 알려진 것이 없다. 최근, ^{18}F-FDG PET / PET-CT은 임상에서 감별진단, 및 수술전 병기결정, 그리고 치료효과를 판정하기 위해 많이 사용되고 있지만, 단지 몇 몇 연구에서만 고형성 가성유두상 종양의 ^{18}F-FDG PET / PET-CT에서의 모양을 연구하였을 뿐, 그 임상적인 영상학적인 패턴을 연구하거나, ^{18}F-FDG의 고강도 섭취를 나타내는 기전에 대한 대사학적인 접근을 보인 연구는 없다.

방법: 고형성가성유두상종양 및 췌장암, 그리고 정상췌장조직 각각 5개 표본에서 당 대사에 필요한 유전자발현을 조사하였으며, p-value가 <0.01이면서, 유전자 발현의 차이가 1.5배 이상인 유전자를 비교 분석하였고, 면역화학염색 및 Western Blot을 이용하여 단백질 발현까지 확인하였다. 고형성가성유두상종양을 췌장절제술을 받은 환자 중 수술전 검사로 ^{18}F-FDG PET / PET-CT를 시행한 환자 36명을 후향적 조사를 하였다. ^{18}F-FDG PET / PET-CT에서의 모양을 전체 종양부피에 대한 ^{18}F-FDG의 고강도 섭취 비율에 따라 Hot-uptake형: ≥70%, Mixed형: 30≤ <70, 그리고 Defective 형: <30%) 세 가지 형

태로 나누었으며, SUV_{max}, SUV_{mean}, $TMV_{2.5}$, 그리고 $TLG_{2.5}$를 조사하여, 당 대사와 관련되어 발현되는 유전자, ^{18}F-FDG의 섭취형태, 그리고, 현미경적 악성도와의 관련성을 분석하였다.

결과: 35명(97.2%)환자가 여자였으며, 1명만이 남자였고, 나이는 34.8±11.2세였다.^{18}F-FDG 섭취형태는 Hot-uptake형(19명), Mixed형 (5명), 그리고 Defective형 (12명)으로 세가지 형태로 분류되었다. 영상의학적 종양의 크기, SUV_{max}, SUV_{mean}, 그리고 $TLG_{2.5}$가 ^{18}F-FDG 섭취형태에 따라 통계학적인 의미가 있는 차이를 보였다(ANOVA, $p<0.05$). 당 대사와 관련된 유전자로서 GLUT1, HK1, PFKM, ENO2, PKM2가 고형성가성유두상종양에서 통계학적인 유의성을 보이는 차이를 보였으며, 이는 면역조직염색법 및 Western Blot에서도 확인할 수 있었다. Defective 형은 다른 형태와 비교해 보았을 때, HK1($p=0.014$), PKM2($P=0.028$), 그리고 Ki-67($p=0.007$)발현이 낮게 관찰되었다. 상대적으로 높은 Ki-67의 발현 (≥3%)은 ^{18}F-FDG의 고강도 섭취를 대변하는 SUV_{max}와 밀접한 관계를 보여 주었다 ($p=0.002$). 또한, Defective형은 현미경적으로도 양성을 나타내는 경향을 보였다 ($p=0.070$). 문헌고찰을 통하여 Hot+Mixed 형은 Defective형과 비교하여 상대적으로 매우 침습적인 양상을 보이는 것으로 분석되었다.

결론: 본 연구는 대사학적인 관점에서 고형성가성유두상종양의 특징을 처음으로 분석한 연구로서, 이 종양은 근본적으로 당 대사능을 높일 수 있는 분자학적인 기전을 가지고 있음을 확인 할 수 있었으며, 이는 임상적으로도 ^{18}F-FDG-PET/PET-CT scan 에서 고강도의 신호로 잘 보이는 이유를 설명할 수 있었다. 따라서, 종양내 출혈 및 괴사의 정도에

따라 세 가지 형태로 임상에서 관찰될 수 있음을 설명할 수 있었으며, Defective 형은 상대적으로 낮은 당 대사능력과 낮은 세포 증식을 보이므로, 환자의 상태에 따라서 수술을 보류하고 지켜볼 수 있는 여지를 제시해 주었다. 향후 서서히 자라는 고형성가성유두상종양과 임상적으로 침습적인 종양간의 대사학적인 차이를 연구하는 것은 매우 흥미로운 과제로 사료되었다.

핵심되는 말: 고형성가성유두상종양, 대사학,

^{18}floro-deoxyglucose positron emission tomography

(^{18}F-FDG-PET), 췌장절제술

PUBLICATION LIST

Kang CM, Kim KS, Choi JS, Kim H, Lee WJ, Kim BR. Solid pseudopapillary tumor of the pancreas suggesting malignant potential. Pancreas 2006;32:276-80.

Kang CM, Kim HK, Kim H, Choi GH, Kim KS, Choi JS, et al. Expression of Wnt target genes in solid pseudopapillary tumor of the pancreas: a pilot study. Pancreas 2009;38:e53-9..

Kang CM, Hwang HK, Kim H, Kim H, Chung YE, Park JS, et al. Marginally calcified totally necrotic tumor of the pancreas: a subset of solid pseudopapillary tumor with near-total necrosis? Pancreas 2013;42:184-6.